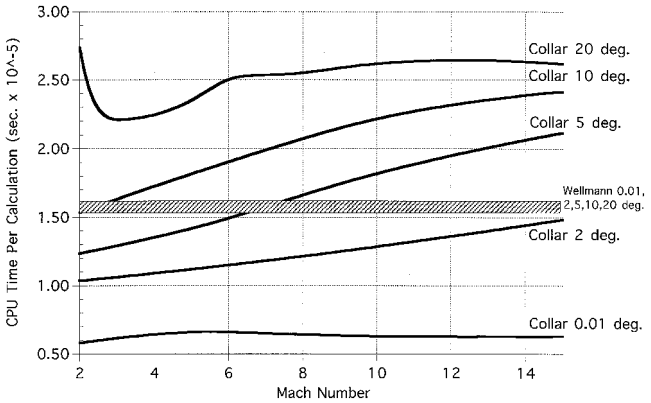

Fig. 2 Sun Sparc20 CPU calculation times of solutions at varying Mach numbers and deflection angles.[1,3]

deg, depending on the Mach number and the Sparc used. Below those angles, Houghton and Brock's method is fastest.

For the DEC Alpha, both closed-form solutions are faster by two to three orders of magnitude over iterative solutions. The closed-form solutions have about the same run-times of around 2.5×10^{-8} s/calculation, which is nearly invariant with Mach number or deflection angle. The iterative solution run-times are dependent on deflection angles and range from 4.3×10^{-6} to 3.8×10^{-5} s/calculation.

On the Cray Y-MP2E/232, closed-form solution run-times are faster, again by orders of magnitude. Run-times for Wellmann's solutions and Mascitti's are 2.9×10^{-9} and 2.4×10^{-7}, respectively, both being invariant with the Mach number and deflection angle. If arrays are not used and the Mach number and deflection angle are initially set, Mascitti's solution can have comparable run-times to Wellmann' solution on the Cray Wellmann's. This is mainly because of the uniqueness of optimization built into the Cray compiler. The iterative solutions have times ranging from 5.0×10^{-6} to 5.6×10^{-5} s/calculation, depending on the deflection angle.

The results for the strong shock solutions are similar to the weak shock solution run-times with the major exception coming from the Sparc machines. Because Wellmann's solution uses only single precision, run-times are reduced by more than half. This makes Wellmann's solution faster than Houghton and Brock's method at any deflection angle and Mach number.

Conclusions

Closed-form solutions of the theta–beta–Mach relationship prove to be faster than iterative solutions for practically all cases on the four machines examined. Note that an exception to this was found when computing the weak shock solution on the Sparc stations for some Mach numbers at deflection angles less than about 5 deg, where Houghton and Brock's method was the fastest. The primary explanation for this is in the number of trigonometric function calls required for each method.

Solving with either of the closed-form solutions requires many trigonometric function calls, which can require substantial CPU time, depending on the individual machine; however, both iterative methods used here also require trigonometric function calls as well as potentially CPU-intensive logic statements. In the secant method, trigonometric functions are used to calculate the maximum deflection angle for one of the initial guess values, and in evaluating the theta–beta–Mach relation during each iteration. Convergence typically requires about five iteration cycles. Compared to the secant method, Houghton and Brock's iteration method has a smaller number of trigonometric function calls per cycle, but may have a larger number of cycles to reach convergence. This method must perform a minimum of two iterations per solution, but the number of iterations generally increases with increasing deflection angles and Mach numbers. For instance, at Mach 10 at a deflection angle of 10 deg, 18 iterations are required to converge on the solution to within a four-decimal-place accuracy with single-precision variables.

Acknowledgment

The authors thank George Emanuel of the University of Oklahoma for bringing these solutions to their attention.

References

[1]Wellmann, J., "Vereinfachung von Rechnungen am schiefen Verdichtungsstoß," *Deutshe Luft- und Raumfahrt*, Forschungsbericht 72-11, Duestche Forschungs- und Verssuchsanstalt für Luft- und Raumfahrt, Institut für Aerodynamik, Brauschweig, Germany, Jan. 1972.

[2]Mascitti, V. R., "A Closed-Form Solution to Oblique Shock-Wave Properties," *Journal of Aircraft*, Vol. 6, 1969, p. 66.

[3]Houghton, E. L., and Brock, A. E., *Tables for Compressible Flow of Dry Air*, 3rd ed., Edward Arnold Ltd., Bungay, Suffolk, England, UK, 1988.

Empirical Model of Transport and Decay of Aircraft Wake Vortices

Lakshmi H. Kantha*
University of Colorado, Boulder, Colorado 80309-0431

Nomenclature

$a_{1,2,3,4}$ = empirical constants
b = wingspan
$c_{1,4,5,6}$ = constants in vortex decay equation
D_1 = distance between the two wake vortices
D_2 = distance between one wake vortex and the image vortex of the other
H = height of the wake vortex center above the ground
L = turbulence length scale
q_* = turbulence velocity scale
R_m = core radius equal to radius of maximum swirl velocity
t = time or age of the vortex
U = wind velocity
u = horizontal velocity of the vortex core
v_m = maximum swirl (tangential) velocity of the vortex
w = vertical velocity of the vortex core
X = horizontal position of the wake vortex center
z = vertical coordinate
α = angle the wind makes with the runway axis
Γ = circulation around the wake vortex
ρ = density of air
σ = vortex tilt parameter

Subscript
i = induced velocity

Introduction

THIS Note expands on a simple empirical model developed earlier for the transport and decay of aircraft trailing (wake) vortices in a turbulent atmosphere near the ground,[1] with potential applications to single and parallel runways. Our approach was similar to that of Greene,[2] but included the

Received Aug. 20, 1997; revision received March 17, 1998; accepted for publication March 24, 1998.

*Professor, Department of Aerospace Engineering Sciences, CB431. E-mail: kantha@colorado.edu. Senior Member AIAA.

ground proximity effects and the influence of ambient turbulence and crosswind shear on the decay rate of the vortices. Well-known Monin–Obukhoff similarity laws in the constant flux region of the lower atmospheric boundary layer were used to compute the ambient shear and turbulence. The model results showed that the proximity of the ground exerts a major influence on vortex decay and transport. However, the model assumed that the circulation around each vortex remains unchanged from its initial value at birth. This represents a highly conservative limit for the vortex pair decay. While the vortex bounce that occurs near the ground was well simulated, vortex-pair tilting[3] and the phenomenon of the lone upwind vortex because of the enhanced decay and disappearance of the downwind vortex[4] were not accounted for. While these estimates are useful as conservative bounds on vortex pair decay and transport, more realistic estimates that account for the decrease in circulation around each vortex by ambient turbulence and wind shear, and even an approximate simulation of vortex pair tilt might be useful.

Traditionally, vorticity in a trailing vortex has been assumed to diffuse steadily outward with the total circulation around it remaining unchanged. This picture is appropriate for an isolated vortex in an infinite quiescent medium. In practice, diffusion of vorticity of the opposite sign across the midplane of the vortex oval can attenuate the circulation around each vortex core. Ambient turbulence can cause detrainment of vorticity from the oval decreasing the circulation around each vortex. In this Note these processes are modeled as processes that decrease the overall circulation around each vortex with a time scale t_s derived from the relevant parameters; $d\Gamma/dt \sim \Gamma/t_s$. For midplane diffusion, the relevant parameters are Γ and D_1, and the time scale $t_s = D_1^2/\Gamma$. For ambient turbulence-induced vortex decay, $t_s = L/q_*$. For ambient shear-induced decay, the natural time scale is $(dU/dz)^{-1}$. The constants of proportionality are, however, highly uncertain and must be chosen empirically from best fit to obervations. Unfortunately, existing high-quality observational data are quite sparse, we therefore confine ourselves to presenting a plausible approach to modeling vortex decay and transport that bears at least a qualitative resemblance to these observations.

Existing observations have shown that vortex oval tilt can be pronounced at times.[3,5] The vortex oval can be taken to have a major axis of length $\sim 1.732b$ and a minor axis $\sim 1.045b$.[6] Vortex oval tilting is suggested to be caused by a shift in the stagnation points on the vortex oval[3] in ambient cross shear involving the parameter $\sigma = 0.25b^2(dU/dz)\sin\alpha/\Gamma$, which is proportional to the ratio of $b(dU/dz)\sin\alpha$ to the induced downwash Γ/b. Therefore, one plausible approach to modeling the vortex-pair tilt may be to introduce an upward velocity proportional to $(dU/dz)\sin\alpha\ b[0.4 - \sigma]$ on the downwind vortex and a downward one of similar magnitude on the upwind vortex. Brashears et al.[3] cite observations that indicate that the downwind vortex is likely to be higher in light shear ($\sigma < 0.4$) and the upwind vortex in high shear ($\sigma > 0.4$).

The ambient crosswind shear not only decreases the circulation around the downwind vortex but also leads to larger downward velocity on it than on the upwind vortex. Under some conditions this can cause it to descend more rapidly than the upwind vortex and lead to vortex-pair tilting.

Empirical Model

For details of the empirical model, the reader is referred to Kantha.[1] The salient difference here is that the circulations around the two vortices are allowed to decay and differ. The crosswind, if any, will be assumed to blow from left to right. When vortex-specific quantities are involved (such as H, X, Γ, u, and w), subscript l refers henceforth to the left (upwind) vortex and r to the right (downwind) vortex. The trailing vortex pair is transported vertically down by the velocity induced at the vortex center by the other member of the pair, and in close proximity to the ground by the induced velocity because of image vortices

$$w_i|_{l,r} = -\Gamma|_{r,l}[(X_r - X_l)/D_1^2 - (X_r - X_l)/D_2^2] \tag{1}$$

The induced horizontal velocity on the vortices is given by

$$u_i|_l = -0.5(\Gamma_l/H_l) + \Gamma_r[(H_r - H_l)/D_1^2 + (H_r + H_l)/D_2^2] \tag{2a}$$

$$u_i|_r = +0.5(\Gamma_r/H_r) + \Gamma_l[(H_r - H_l)/D_1^2 - (H_r + H_l)/D_2^2] \tag{2b}$$

for the left and right vortices, with the observer facing the aircraft. In the presence of a crosswind, the total horizontal velocity is $(u_i)_{l,r} + U(z)\sin\alpha$. The height of the wake vortex above the ground can be written as

$$\frac{dH_l}{dt} = (w_i + w_s + w_c)_l - a_4 b\left(\frac{dU}{dz}\right)_{av}\sin\alpha\,(0.4 - \sigma) \tag{3a}$$

$$\frac{dH_r}{dt} = (w_i + w_s + w_c)_r + a_4 b\left(\frac{dU}{dz}\right)_{av}\sin\alpha\,(0.4 - \sigma) \tag{3b}$$

where σ is based on the average of the wind shear and circulation of the two vortices. $w_s = a_3\Gamma/H$ parameterizes the vortex bounce near the ground and, w_c is the effect of heated runway[1]; $a_3 \sim 0.06$, $a_4 \sim 0.3$. The last term parameterizes the influence of ambient shear on the vortex oval that can lead to vortex pair tilt. The horizontal position of the vortices perpendicular to the runways is given by $dX_{l,r}/dt = (u_i)_{l,r} + U(z)\sin\alpha$, with the origin located at the center of the left runway.

The principal difference from Kantha[1] is that only the self-diffusion of the maximum core swirl velocity $v_m = 0.5\Gamma/R_m$ is parameterized as a function of time by $dv_m/dt = -c_l(\Gamma/R_m^2)v_m$. But the circulation is allowed to decay and the decrease in the circulation of each vortex resulting from the diffusion of vorticity of the opposite sign by the other vortex, because of ambient turbulence, and in the case of the downwind vortex by ambient wind shear, is parameterized as

$$\frac{d\Gamma_l}{dt} = -\left[c_4\left(\frac{\Gamma_r}{D_1^2}\right) + c_5\left(\frac{q_*}{H_l}\right)\right]\Gamma_l \tag{4a}$$

$$\frac{d\Gamma_r}{dt} = -\left[c_4\left(\frac{\Gamma_l}{D_1^2}\right) + c_5\left(\frac{q_*}{H_r}\right) + c_6\left(\frac{dU}{dz}\right)\sin\alpha\right]\Gamma_r \tag{4b}$$

In the constant flux part of the atmospheric boundary layer adjacent to the ground, $L \sim H$. The buoyancy effects that retard the vortex oval descent[2] are of secondary importance in the vicinity of the ground and are therefore ignored.

Kopp[5] presents continuous wave Doppler lidar measurements of trailing vortices for B747 and other classes of aircraft at Frankfurt/Main that are helpful in model formulation. His observations show wake vortices to decay to nondangerous state in $\sim$120–140 s for all classes of aircraft. This nondangerous state is arbitrarily defined by Kopp as the state when the maximum swirl velocity in the vortex is below 4 m/s. The decay can however be faster and in as little as 60 s. Empirical constants c_1, c_4, c_5, and c_6 have been chosen to yield results qualitatively consistent with Kopp's observations: $c_1 \sim 0.006$, $c_4 \sim 0.6$, $c_5 \sim 0.3$, $c_6 \sim 2.0$.

Observations show that there exists an initial roll-up phase, when the maximum swirl velocity remains roughly constant or even increases slightly. This phase lasts for 20–40 s after birth.[5] Relevant parameters during this phase are Γ and b, and the only time and space scales that can be formed from these are $t_R = b^2/\Gamma$ and b. The roll-up time of the vortex can be taken as proportional to t_R and the initial vortex core size as proportional to b. The circulation changes very little during this phase, the vorticity is more tightly wound and the core radius decreases slightly, leading to a slight increase in the maximum velocity. The model accounts for these effects by requiring that

the circulation around each vortex remain unchanged for a time equal to t_R, while the vortex core size decreases from $0.06b$ to $0.05b$ over this time. Past the roll-up phase, the equations are integrated as in Kantha[1] to determine the position in space and the strength of the wake vortices at any given time. At $t = 0$, the vortices are assumed to be spaced by a distance equal to $0.8b$ and located symmetrically on either side of the center of the runway at height H_0, and $\Gamma_{l,r} = \Gamma_0$, the circulation around the bound vortex.

Model Results

To illustrate the various influences of ambient conditions on the vortex pair decay and transport close to the ground, consider a B747-300 (weight ~260,000 kg, wingspan ~60 m). Landing speed is assumed to be 60 m/s and the wind is assumed to blow at 30 deg to the runway, leading to a crosswind of half that value. Five different cases are considered: 1) Zero ambient wind and neutral stratification, 2) zero ambient wind but daytime convective conditions (with a heat flux from the ground of 100 W/m^2), 3) light ambient shear from a 3 m/s wind under neutral stratification, 4) high ambient shear with 10 m/s wind under neutral stratification conditions, leading to significant crosswinds (5 m/s) and shear, and 5) 5-m/s wind and nighttime stably stratified atmospheric boundary-layer conditions (with a heat flux of 5 W/m^2 to the ground). Case 1 highlights the vortex pair evolution under quiescent conditions in the absence of external influences. Case 2 allows consideration of the influence of ambient turbulence on vortex decay. Cases 3 and 4 bring ambient crosswind shear and shear-generated ambient turbulence into the picture, with the high shear case, case 4, causing rapid decay of downwind vortex. Case 5 simulates nighttime stably stratified but windy conditions that can lead to strong shear near the ground. If the stability is too large, such as during windless cloud-free nights, ambient turbulence is extinguished.

Figure 1 shows the evolution in time of the circulation, the self-induced horizontal velocity, and the maximum swirl velocity in each vortex core for a B747 for all five cases with $H_0 = 50$ m. The scaling for the initial vortex radius chosen appears to yield reasonable numbers for the initial values of v_m. Note the small initial increase in the maximum swirl velocity during the roll-up phase. The magnitudes and rates of change of the self-induced horizontal and maximum swirl velocities are qualitatively consistent with those presented by Kopp.[5] Case 1 involves no shear and no ambient turbulence and, hence, the decrease in circulation is a result of only cross diffusion of vorticity. The decay and motion of the two trailing vortices are similar to that in Kantha[1]; there is symmetry about the vortex oval center. The degree of the vortex bounce is qualitatively similar to that presented in Kopp.[5] After the initial phase the circulation around each vortex decreases to about 80% of the initial value, and once the vortices move far apart it ceases to decrease further. Case 2 involves ambient turbulence generated by convective heating and, hence, the vortex decay is accelerated by erosion of vortex oval by turbulent eddies. The circulation around both vortices decreases more rapidly and steadily. Symmetry still prevails. Case 3 involves wind-shear-generated ambient turbulence, as well as crosswind shear. This then produces both accelerated decay of downwind vortex as well as vortex-pair tilt. The shear is light enough for the downwind vortex to remain more or less intact. Case 4, however, involves high shear that leads to a rapid decay and disappearance of the downwind vortex. The upwind vortex remains more or less intact even though its circulation decreases because of ambient turbulence. The upwind vortex is also generally lower than the downwind one under these conditions. Case 5 is essentially similar to case 4, but the higher shear (for the same wind conditions) produced by atmospheric stability causes even more rapid decay of the downwind vortex. Under strong stable stratification and weak winds, turbulence is extinguished, the ambient conditions become quiescent

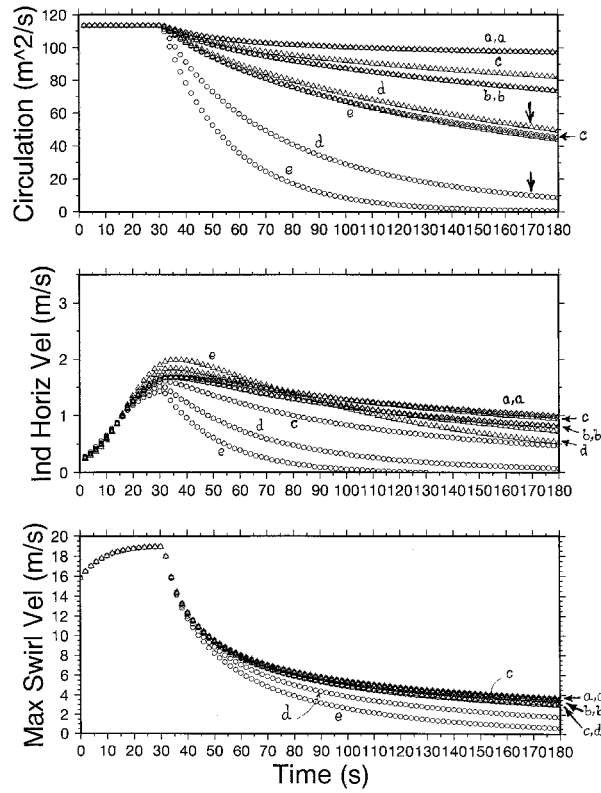

Fig. 1 Circulation, the induced horizontal velocity and the maximum swirl velocity in the vortex core as a function of time for cases 1–5. △, upwind vortex; ○, downwind vortex. Note the initial rollup and the final decay phases. Symbols a, b, c, d, and e correspond to cases 1, 2, 3, 4, and 5, respectively.

and one recovers case 1 conditions in the model, because the buoyancy forces on the vortex oval caused by ambient stratification are ignored in the model. However, in practice, stable ambient stratification tends to retard the descent of the vortex oval (conversely, any daytime unstable stratification near the ground tends to accelerate the descent of the oval). Using the Monin–Obukhoff theory, these effects can be included in the model if needed.

Because both the maximum swirl velocity and circulation are modeled, either or both can be used to characterize the severity of the vortex wake encounter. Note that while maximum swirl velocity may not be a plausible measure of the severity of wake encounter, a more appropriate one might be the circulation $\Gamma_{1/2}$ at a radius equal to the half-span of the trailing aircraft, because this represents the rolling moment induced on it in a vortex encounter. In addition, one needs to allow for the characteristics of the following aircraft. One possible nondimensional wake encounter severity parameter is $K = [\Gamma_{1/2}/\Gamma_F] = (b_F/b_L)(M_L/M_F)(v_m b_F)^2[\Gamma_F^2 + (v_m b_F)^2]^{-1}$, where subscripts L and F denote the leading and following aircraft, respectively. Neither v_m nor M_L/M_F by itself is likely to adequately characterize the severity of a vortex wake encounter. K can be obtained from the preceding solutions.

Trailing vortices often decay from Crow sinusoidal instability[7] or bursting.[8] These modes are the primary mechanisms for vortex decay for a trailing vortex pair far away from the influence of the ground. The time for the vortex pair to decay in the free atmosphere because of the Crow instability is often taken as the time for the vortices to touch each other and observations indicate that it is roughly equal to $0.8b\ (l/b)^{1/3}/q_*$.[2,7] This estimate is consistent with dimensional considerations because the only time scale that can be formed from b and q_* is b/q_*, and the time scale for Crow instability should be proportional to this. For extension to proximity of the ground, where the turbulence length scale can be well approx-

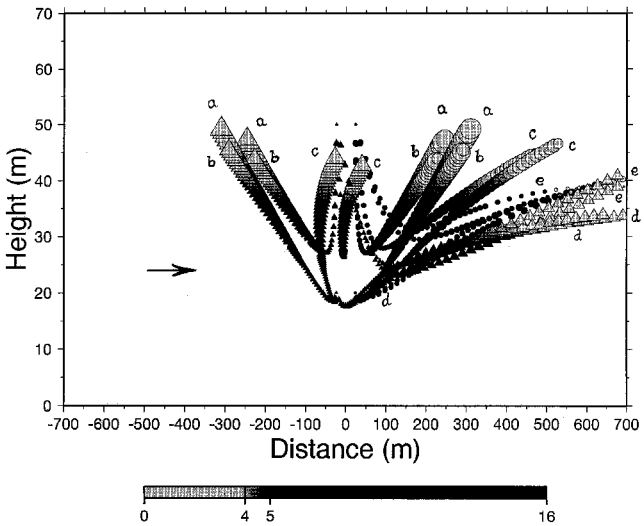

Fig. 2 Position of the upwind (△) and downwind (○) vortices for all five cases. ●, maximum swirl velocities >4 m/s; and ○, <4 m/s. The size of the circle is proportional to the core radius. Symbols a, b, c, d, and e correspond to cases 1, 2, 3, 4, and 5, respectively.

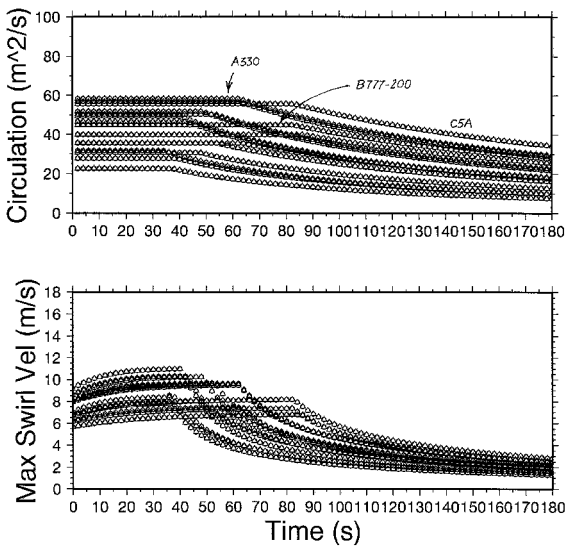

Fig. 3 Circulation and the maximum swirl velocity in the vortex core as a function of time for various aircraft flying at 9000-m height. △, the upwind vortex; ○, downwind vortex. Note the longer initial rollup phase.

imated by κz (where κ is von Kármán constant) and where the vortex spacing is not constant, $\int [q_*/(\kappa z)^{1/3}]dt$ must equal or exceed $D_1^{2/3}$, for the vortices to decay by this mechanism. This condition is not always satisfied because after the nearly vertical initial descent, the vortices begin to move apart fairly rapidly. However, in ambient shear conditions, the time scale for Crow instability may be reached well before the vortices decay. These times are shown by an arrowhead in Fig. 1. Vortex bursting may also be important, although for a conservative estimate of vortex lifetime, it may be ignored.

Figure 2 shows the trajectories of the two vortices for two values of H_0: 1) 50 m and 2) 20 m. The positions of the upwind and downwind vortices are shown looking head-on toward the landing aircraft, every 2 s for the first 60 s and 5 s afterward. The size of the circle is proportional to the vortex core radius. The wind is from the left. Filled circles indicate hazardous levels of the maximum swirl velocity defined quite arbitrarily as 4 m/s (note that the circulation remains high in some cases even after 3 min). Vortex tilt can be seen for strong shear cases. The wake vortices appear to predominantly populate the space between 15 and 45 m above the ground, once again qualitatively consistent with lidar observations by Kopp.[5]

Simulations for a B757 (weight ~90,000 kg, wingspan ~38 m) for a variety of ambient conditions, and two initial heights, H_0 = 20 and 50 m, and a landing speed of 60 m/s are similar. Generally speaking, for a given aircraft, quiescent ambient conditions are the most hazardous because the vortex decay is then slow. Light crosswinds tend to exacerbate this by promoting the tendency of the upwind vortex to loiter in the vicinity of the runway at heights comparable to that of succeeding aircraft. Crosswinds are however more hazardous to flight operations on a parallel runway spaced closer than about 500–600 m. Then both vortices tend to get transported to the vicinity of the parallel runway at a height comparable to that of the landing aircraft.

Finally, the model can be readily applied to aircraft flying far above the ground influence. Figure 3 shows the circulation and maximum swirl velocity as a function of time for the aircraft listed in Table 1 of Kantha.[1] The cruise altitude is taken to be 9000 m, the cruise speed 250 m/s, the ambient air density as 0.5 kg/m^3 (as opposed to 1.25 kg/m^3 at sea level). The ambient turbulence velocity scale is taken as 0.5 m/s, and the turbulence length scale as 100 m. Because of the lower circulations, the roll-up phase lasts longer. The vortices descend about 120–150 m in 3 min; by that time, while the swirl velocity drops below 4 m/s, the circulation remains high, in some cases posing a potential hazard unless the Crow instability or bursting can destroy the coherence of the vortex core. For the chosen parameters the Crow instability time scale is 80–100 s. Note that for these short descent distances and times, the buoyant retardation of the vortices has been neglected.[2]

It is our hope that the data being currently gathered under the NASA Terminal Area Productivity program would be helpful in calibrating this model and refining it.[9]

Concluding Remarks

An earlier empirical model of the transport and decay of aircraft wake vortices has been extended to include the effect of the decrease in the vortex circulation caused by ambient turbulence and shear, the shear-induced tilt of the vortex oval, and the initial roll-up phase. In addition to simulating the vortex bounce frequently observed near the ground, the model is now formulated to simulate the accelerated decay of the downwind vortex in crosswind shear, which often leads to the phenomenon of a lone surviving vortex. The ambient crosswind shear produces a vortex pair tilt with the downwind vortex being higher at normal crosswind speeds. Quite high crosswinds are needed to tilt the vortex in the other direction, where the upwind vortex is higher.

Recall that the various processes affecting wake vortex decay and transport are only approximately modeled, and there is considerable uncertainty in the values of the empirical model constants. Quantitative and self-complete observational data under carefully selected, or at least well-measured, ambient conditions would be of great help in not only understanding these processes, but also parameterizing them in a simple empirical model such as this. Sustained monitoring of wake vortices and ambient conditions at a few airports by Doppler lidar is highly desirable in enabling more efficient yet safe flight operations to be conducted at busy airports around the world.

References

[1]Kantha, L. H., "Empirical Model of Transport and Decay of Wake Vortices Between Parallel Runways," *Journal of Aircraft*, Vol. 33, No. 4, 1996, pp. 752–760.

[2]Greene, G. C., "An Approximate Model of Vortex decay in the Atmosphere," *Journal of Aircraft*, Vol. 23, No. 7, 1986, pp. 566–573.

[3]Brashears, M. R., Logan, N. A., and Hallock, J. N., "Effect of Wind Shear and Ground Plane on Aircraft Wake Vortices," *Journal of Aircraft*, Vol. 12, No. 10, 1975, pp. 830–833.

[4]Bilanin, A. J., Teske, M. E., and Hirsh, J. E., "Neutral Atmospheric Effects on the Dissipation of Aircraft Vortex Wakes," *AIAA Journal*, Vol. 16, No. 9, 1978, pp. 956–961.

[5]Kopp, F., "Doppler Lidar Investigation of Wake Vortex Transport Between Closely Spaced Parallel Runways," *AIAA Journal*, Vol. 32, No. 4, 1994, pp. 805–810.

[6]Corjon, A., and Poinsot, T., "A Model to Define Aircraft Separations Due to Wake Vortex Encounter," AIAA Paper 95-1776, June 1995.

[7]Crow, S. C., and Bate, E. R., "Lifespan of Trailing Vortices in a Turbulent Atmosphere," *Journal of Aircraft*, Vol. 13, No. 7, 1976, pp. 476–484.

[8]Liu, H.-T., "Effects of Ambient Turbulence on the Decay of a Trailing Vortex Wake," *Journal of Aircraft*, Vol. 29, No. 1, 1992, pp. 255–263.

[9]Perry, R. B., Hinton, D. A., and Stuever, R. A., "NASA Wake Vortex Research for Aircraft Spacing," AIAA Paper 97-0057, Jan. 1997.

Low-Reynolds-Number Effects on Delta-Wing Aerodynamics

Lance W. Traub,* Brian Moeller,†
and Othon Rediniotis‡
Texas A&M University,
College Station, Texas 77840-3141

Introduction

FLOW visualization has traditionally provided a powerful technique for both qualitative and quantitative investigations of delta-wing flows. Because low-speed water flows are conducive to flow visualization techniques, many studies have addressed low Reynolds number (*Re*) flow. Some examples are the investigations of Atta and Rockwell[1] at $Re = 5.8 \times 10^3$, Reynolds and Abtahi[2] at a *Re* between 1.9×10^4 and 6.5×10^4, Traub et al.[3] with *Re* in the neighborhood of 9×10^3, and Lowson[4] at *Re* as low as 6.6×10^3 (performed in a wind tunnel). However, accompanying pressure, force, and moment measurements have typically been performed at significantly higher *Re* because of sensitivity and accuracy limitations of typical pressure and load measurement instrumentation at low dynamic pressures. Most pressure and load measurement efforts have been performed at *Re* above 0.34×10^6.[5–7] The presence of this *Re* gap raises the question of flow sensitivity, particularly in the range from 10^4 to 10^5. How reconcilable are the two data sets, i.e., flow visualization data and pressure/load data? Do they describe the same flow patterns?

A compilation of data by Erickson,[8] taken from water and wind-tunnel tests as well as in flight, and spanning a *Re* range from 9.8×10^3 to 4.0×10^7, indicate that vortex location and breakdown are governed by an inviscid mechanism. Lowson[4] compared vortex core positions for a range of *Re* (between 6.6×10^3 and 1.6×10^6). Significant scatter existed in the data. He suggested that although the results appear to justify low *Re* studies of high *Re* delta-wing flows, care should be applied in certain areas in extrapolating from low to high *Re*. Roos and Kegelman[9] investigated the influence of sweep angle on delta-wing flows and concluded that vortex core trajectories, vortex burst locations and wing lift show no significant sensitivity to *Re* changes. However, the *Re* for their tests ranged between 0.34×10^6 and 2.0×10^6. A slight decrease of the maximum lift was observed with increasing *Re*. Exceptions to the practice of avoiding pressure and load measurements at low *Re* are the investigations of Lee et al.[10] ($Re = 2.3 \times 10^4$) and Gursul and Ho[11] (*Re* between 3×10^4 and 6×10^4). Lift data by Lee et al. indicate that the aerodynamic forces on delta wings are insensitive to *Re*. They also suggested that for sharp-edged wings the vortex breakdown location is independent of *Re*. A study has been undertaken to elucidate if the local flow features and the integrated coefficients are sensitive to low *Re* effects. Consequently, in this Note, an investigation of the effect of *Re* from 2×10^4 to 6×10^4 on delta wings is described. The study contains force balance, pressure, and hot-wire anemometer measurements, and on and off-surface flow visualization.

Experimental Equipment

The wind-tunnel models were manufactured from 1.27-mm aluminum plate and had a root chord, *c*, of 100 mm, giving a wing thickness-to-chord ratio of 1.27%. Two models were manufactured with leading-edge sweep angles, Λ, of 60 and 70 deg, respectively. The wing's leading and trailing edges were square edged. The 60-deg sweep delta was pressure tapped, with a row of 14 tappings spaced 2 mm apart located at 60% of the wing root chord (Fig. 1). An Air Neotronics autozeroing digital manometer was used to measure the pressure. This manometer can resolve pressures down to 0.1 Pa. The manometer was sampled 500 times using a 16-bit A/D board and then averaged.

The wind-tunnel tests were undertaken in a 1×1-ft low-turbulence wind tunnel. The maximum blockage for the two wings based on the projected frontal area was 3.9 and 2.7% for the $\Lambda = 60$- and 70-deg wings, respectively. The results that are presented do not include blockage or upwash corrections to avoid potentially contaminating the data. The omission of corrections (whose correct application for wings with vortical flow, particularly in flows involving vortex breakdown is uncertain) is also justifiable as the level of blockage is low. A SETRA force balance was used to measure lift. The balance has a resolution of 0.01 g.

Water-tunnel tests were undertaken in a 2×3-ft tunnel. Wing's, geometrically similar to the wind-tunnel models were manufactured for water-tunnel flow visualization, with a root chord of 200 mm. The chord of the water-tunnel models was selected to ensure that upwash effects should be equivalent for both test facilities. Measurements were also taken over the wing using a TSI 1051-2 hot-wire Anemometer system. Data

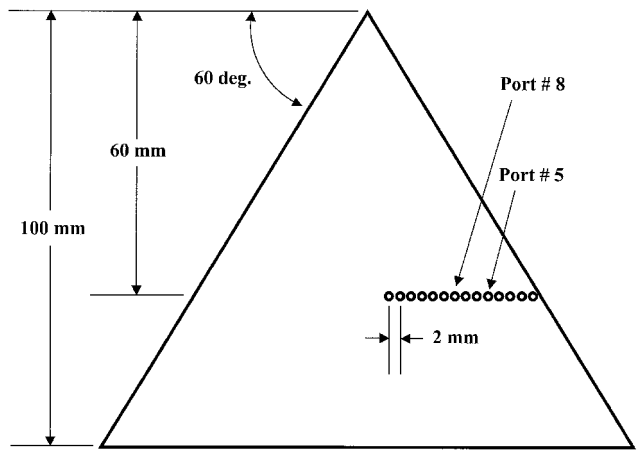

Fig. 1 Model pressure tapping details.

Received Nov. 23, 1997; revision received March 31, 1998; accepted for publication March 31, 1998.

*Graduate Student, Aerospace Engineering Department. Associate Member AIAA.

†Graduate Student, Aerospace Engineering Department. Student Member AIAA.

‡Assistant Professor, Aerospace Engineering Department. Member AIAA.